THERMOCHEMICAL MODELLING OF FLUID-ROCK REACTIONS IN VERA RUBIN RIDGE, GALE CRATER, MARS. S.M.R. Turner[1], S.P. Schwenzer[1], J.C. Bridges[2], C.C. Bedford[1], E.B. Rampe[3], A.A. Fraeman[4], A. McAdam[5], N. Mangold[6], J. L'Haridon[6]. [1]The Open University, UK, (stuart.turner@open.ac.uk). [2]The University of Leicester, UK. [3]NASA Johnson Space Center, USA. [4]Jet Propulsion Laboratory, California Institute of Technology, USA. [5]NASA Goddard Space Flight Center, USA. [6]Laboratoire de Planétologie et Géophysique de Nantes, Université de Nantes, France.

Introduction: Vera Rubin Ridge (VRR) in Gale Crater, Mars, is a ~200 m wide ~6.5 km long northeast-southwest resistant geomorphological feature on the northern slopes of Aeolis Mons (Mt. Sharp). Analysis of Compact Reconnaissance Imaging Spectrometer for Mars (CRISM) orbital data showed that VRR has strong hematite spectral signatures [1]. Hematite was confirmed in-situ at VRR with the *Curiosity* rover [2,3] and has been shown to be present throughout the Murray formation [4–7]. VRR is stratigraphically continuous with the underlying Murray formation [8,9].

Previous thermochemical modelling showed how hematite at VRR could have formed as the result of open-system weathering at high water/rock ratios [10]. Here we use thermochemical modelling to investigate possible reaction pathways for the hematite-clay-bearing assemblage observed at VRR, starting from an identified least-altered (minimum clay content) Murray composition, and a Mars basal brine [11,12].

Modelling method: We used CHIM-XPT software to conduct thermochemical modelling [13]. CHIM-XPT is a program for computing multicomponent heterogeneous chemical equilibria in aqueous-mineral-gas systems, and has been previously used to model fluid-rock reactions at Gale crater [10–12]. Every calculation step calculates equilibrium between the fluid and the dissolved rock, meaning that each step can be treated and interpreted independently from the direction from which it was reached. In CHIM-XPT, the water/rock ratio (W/R) is the ratio of incoming fluid to reacted rock. The models here focus on 1–100,000 W/R.

The Starting Fluid. Gale Portage Water (GPW) [11] was selected as the starting fluid, as this fluid was derived from equilibrium mediation between a brine and rocks of the Gale area. The solution is initially oxidizing (all S species as SO_4^{2-}), and the redox in the fluid is controlled by the SO_4^{2-}/HS^- pair. The redox of the system throughout each model is dependent on the Fe^{2+}/Fe^{3+} ratio of the host rock. pH was modelled as a free-parameter throughout.

The Starting Rock. The initial starting composition was selected from Murray drill sample compositions that are mineralogically least altered, based on clay content (assuming the clays are authigenic). The Telegraph Peak (TP) drill sample was found to be most statistically representative of a bulk lower Murray composition based on a comparison to the average

APXS compositions of the Confidence Hills, Mojave 2 and TP CheMin samples [7]. Furthermore, ChemCam bulk contour analysis [14] showed TP to be nearest the overall mean Murray composition. Based on these analyses, TP compositions [7] were selected for the initial starting compositions in our modelling.

Results: Initial modelling focused on establishing a 'parameter space' where the bulk, crystalline and amorphous components of TP [7] were reacted with GPW [11]. Modelling progressed to investigate different dissolution scenarios. Guided by relative mineral solubility [15], we investigated dissolving TP amorphous and olivine [7]. We then progressed to mixtures of olivine, TP amorphous and TP crystalline [7] to adjust for the lack of Al in the resulting mineral phases compared to VRR drill samples [2,3].
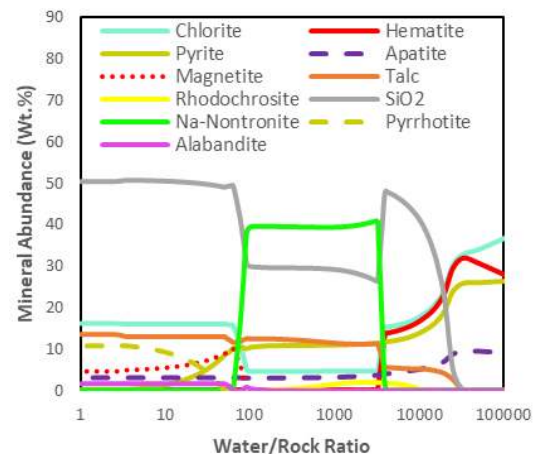

Fig. 1: CHIM-XPT thermochemical model for the reaction of the amorphous component of TP [7] and GPW [11]. The model was run at 50 °C and 0.1 Fe^{3+}/Fe_{total}.

Initial 'Parameter Space' Modelling. This focused on modelling the individual bulk, crystalline and amorphous components of TP [7] with GPW [11] over a range of temperatures (20 °C, 50 °C, and 100 °C). The total Fe in the starting composition was expressed in various amounts of Fe^{2+} and Fe^{3+} (100% Fe^{2+}, 90% Fe^{2+} & 10% Fe^{3+}, 50% Fe^{2+} & 50% Fe^{3+}).

The bulk composition of TP failed to produce any Fe-oxide at 20 °C and 50 °C, but did produce hematite at 100 °C for >100,000 W/R.

The crystalline composition of TP only produced Fe-oxide at 0.5 Fe^{3+}/Fe_{total}, with goethite precipitating at 20 °C (<10 wt.% for ~5,000–100,000 W/R) and

hematite precipitating at 50 °C (<10 wt.% ~8,000–100,000 W/R) and 100 °C (<10 wt.% 1,000–100,000 W/R with trace amounts down to ~50 W/R).

The amorphous composition of TP produced significant amounts of Fe-oxide. At 20 °C, >10 wt.% goethite precipitated between 12,000–100,000 W/R. At 50 °C, >10 wt.% and up to ~30 wt.% hematite precipitates between 5,000–100,000 W/R (Fig. 1). At 100 °C >30 wt.% hematite precipitates between 10,000–100,000 W/R for all modelled Fe^{2+}/Fe^{3+} ratios.
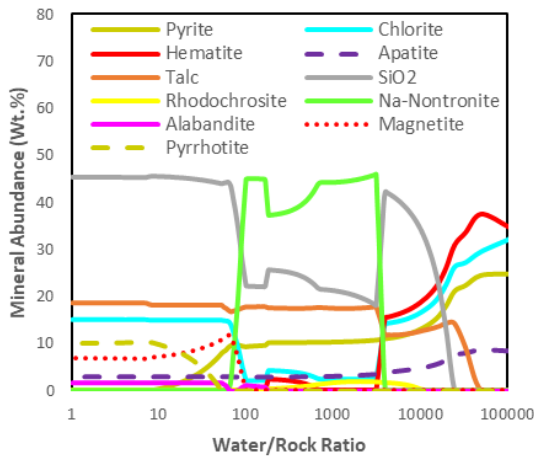

Fig. 2: CHIM-XPT thermochemical model for a starting composition of 94% olivine and 6% TP amorphous [7] and GPW [11]. The model was run at 50 °C and 0.1 Fe^{3+}/Fe_{total}.
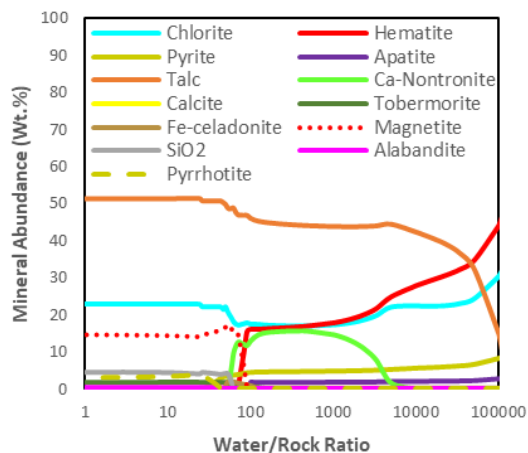

Fig. 3: CHIM-XPT thermochemical model for a starting composition of TP amorphous (30%), TP crystalline (20%) and olivine (50%) [7], and GPW [11]. The model was run at 50 °C and 0.1 Fe^{3+}/Fe_{total}.

Olivine and TP Amorphous Starting Composition. Comparisons of the TP [6,7] and VRR [2,3] CheMin mineralogies showed that olivine is present in TP but not in Stoer, Highfield or Rock Hall (Morris et al., *this conference* [2]). Considering olivine is very reactive, and thus may have been a component that has been dissolved, we decided to mix olivine and the amor-

phous component, in the same proportions that they occur in TP [7]. Fig. 2 shows the result of this starting composition reacting with GPW, which shows an increase in hematite wt.% between 5,000–100,000 W/R compared to Fig. 1, and a ~2 wt.% hematite precipitating between 100–1,000 W/R that corresponds to an increase in SiO_2 wt.%.

Olivine, TP Amorphous and TP Crystalline Starting Compositions. The next iteration of modelling focused on mixing olivine with both the crystalline and amorphous components of TP [7]. Fig. 3 shows one starting composition mixture reacting with GPW, resulting >10 wt.% hematite precipitating between 100–100,000 W/R peaking at ~44 wt.% at 100,000 W/R.

Discussion: The models presented here indicate a potential formation process for the hematite-clay assemblage at VRR/Murray of alteration of precursor silicate materials by an oxidizing fluid at temperatures ≥50 °C. In comparison, previous hypotheses for hematite formation at VRR include oxidation of an anoxic Fe^{2+} rich fluid resulting in deposition of hematite [1,16], and alteration of sediments in the shallows of a redox-stratified ancient lake [17].

Our thermochemical modelling assumes that the presently observed mineralogy is what was precipitated. However, it is possible that goethite initially precipitated and underwent phase transition to hematite over time [18]. Furthermore, the presence of talc in Figs. 1–3 is not observed in drill-hole compositions to date, and presence of jarosite and akaganeite in Stoer and Rock Hall [2] is not currently explained by our models. Further work will be undertaken to refine the predicted mineral assemblages and to include reaction pathways that lead to sulfate and oxide precipitation.

Summary: Thermochemical modelling of the reaction between TP compositions [7] and GPW [11] has showed that hematite is readily produced at >100 W/R and 50 °C, for all modelled Fe^{2+}/Fe^{3+} ratios. This suggests that the hematite at VRR could have been a conduit for groundwater flow at temperatures ≥50 °C.

References: [1] Fraeman A.A. et al., (2013) *Geology*, *41(10)*, 1103-1106. [2] Morris R.V. et al., (2019) *LPSC*, *50*, (*this conf.*). [3] Bristow T.F. et al., (2018) AGU Abstract P41A-01. [4] Bristow T.F. et al., (2018) *Sci. Adv.*, *4*, eaar3330. [5] Fraeman A.A. et al., (2019) *LPSC*, *50*, (*this conf.*). [6] Rampe E.B. et al., (2017) *EPSL*, 471, 172-185. [7] Morrison S.M. et al., (2018) *Am. Min.*, *103*, 857-871. [8] Edgar L.A. et al., (2018) *LPSC*, *49*, #1704. [9] Edgar L.A. et al., (2018) AGU Abstract P41A-01. [10] Bridges J.C. et al., (2015) *LPSC*, *46*, #1769. [11] Bridges J.C. et al., (2015) *JGR: Planets*, *120*, 1-19. [12] Schwenzer S.P. et al., (2016) *MAPS*, *51*(11), 2175-2202. [13] Reed M.H. et al., (2010): Users Guide for CHIM-XPT; 71p.; Oregon (University of Oregon). [14] Bedford C.C., (2019) PhD thesis (*in prep*), The Open University, UK. [15] Gudbrandsson S. et al., (2011) *GCA*, *75*(19), 5496-5509. [16] Fraeman A.A. et al., (2016) *JGR: Planets*, *121*, 1713-1736. [17] Hurowitz J.A. et al., (2017) *Science*, *356*, eaah6849. [18] Cornell R.M. and Schwertmann U., (2003) *The Iron Oxides*. Wiley and Sons.